Ionics
https://doi.org/10.1007/s11581-020-03592-8

ORIGINAL PAPER

Stable prismatic layer structured cathode material via Cation mixing for sodium ion battery

P. Arjunan[1] · M. Kouthaman[1] · K. Kannan[1] · K. Diwakar[1] · R. Subadevi[1] · S. Raghu[2] · M. Sivakumar[1]

Received: 10 January 2020 / Accepted: 20 April 2020

Abstract

Recently, P2-type (prismatic site) and O2 (octahedral site)/P2-type materials like $Na_{0.66}Fe_{0.33}Mn_{0.5}O_2$ exhibit favorable capacities more than its theoretical value (173 mAh g^{-1}). However, their low operating potential window ≤ 3 V makes them not desirable for practical applications. Among the sodium (Na) cathodes, the P2-Na-Ni-Mn-O is a significant material because of its high theoretical capacity of ≤ 250 mAh g^{-1} even if it undergoes severe voltage decay with capacity fade due to stacking faults upon cycling above the cut-off voltage (≥ 4.2 V). En route to evade this problem, we substitute zinc (Zn) cation into the P2-Na-Ni-Mn-O system as structure stabilizer, and this material delivers high initial discharge capacity of 205 mAh g^{-1} while cycling in the range 1.5 to 4.5 V. The X-ray diffraction pattern, energy dispersive spectroscopy (EDS) with mapping, and XPS results show that Zn^{2+} befit in to the P2-layer structure of Na-Ni-Mn-O2 without changing its origin.

Keywords P2-layer material · Cation mixing · High-voltage cathode · Na-ion battery

Introduction

Currently, in the worldwide electric vehicle (EV) sectors, portable electronic devices are powered by only lithium ion technology. So, it leads the lithium resources into rich demand with high cost [1–3]. We are in the need of long-range EVs by means of high performance with fast charging batteries [4–6]. The lithium distribution around the globe is too little when compared with the current need. The research community all over the place is seeking an alternative for lithium by focusing on low-cost energy storage technology with highly abundant materials, viz., sodium (Na). In this way, the work towards the sodium is resumed after few decades, owing to the same electrochemical properties like lithium [7, 8].

In the development of large scale sodium ion battery (SIB), the electrode materials are in need of reinforcing to deliver high capacity with long-lasting life. There is large number of cathode materials reported for SIBs with various crystal structures including all type of layers [9–12]. In particular, the layered Na_xMO_2 (M = Mn, Fe, Ni, and Co) has been considered as a promising electrode material for development of Na-ion batteries due to their high theoretical capacity ≤ 250 mAh g^{-1}. Fundamentally, the layered-type materials were classified into two types such as prismatic (P2) and octahedral (O3) based on the stacking of Na-ion in between the transition metal layers. P2-type layer structure is the more promising one for larger radius Na-ion during the intercalation process [13]. The recent reports on P2-type cathodes based on $Na_{2/3}Fe_{1/2}Mn_{1/2}O_2$ and P2-type Na-Ni-Mn-O described the existence of high capacity around 180 mAh g^{-1}, but these materials can operate only at very low voltage range (≤ 3.8 vs Na). Hence, these are not suitable for practical applications. Moreover, they exhibit severe capacity fade with huge voltage decay within fewer cycles while cycling at large voltage window (≥ 4.2 V), which is due to P2-O2 phase evolution by Jahn-Teller effect [14, 15].

There are many strategies such as surface modification by oxides (Al_2O_3) [16], phosphate coatings ($CoPO_4$) [17], and

Electronic supplementary material The online version of this article (https://doi.org/10.1007/s11581-020-03592-8) contains supplementary material, which is available to authorized users.

✉ R. Subadevi
susimsk@yahoo.co.in

✉ M. Sivakumar
susiva73@yahoo.co.in

[1] Department of Physics, Alagappa University, #120, Energy Materials Lab, Science Block, Karaikudi, Tamil Nadu 630003, India

[2] Centre for Advanced Research and Development (CARD), Vels Institute of Science, Technology and Advanced Studies (VISTAS), Chennai, Tamil Nadu 600117, India

Published online: 22 May 2020

cation substitution method, which were proposed to overcome the mentioned issues of the materials. In the midst of them, the cation substitution is an effective way for the P2-Na-Ni-Mn-O system, where the cation act as a stabilizer to uphold the crystal structure by controlling the lattice parameters during phase evolution at higher operating voltage. In addition, the cation substitution is classified into two types, viz., electrochemically (i) active—Co and Fe; and (ii) inactive—Li and Ti [18–22], based on the redox activity of the transition metals during the high voltage operation.

Sequentially, herein we have successfully prepared the Zn-substituted P2-type $Na_{0.66}Ni_{0.33-x}Zn_{1-x}$ $Mn_{0.67}O_2$ material via conventional solid state method. Latter, complete studies on structural, morphological, and electrochemical properties of the proposed materials were carried out, and the results were discussed.

Experimental

Material preparation

The stabled Zn-substituted P2-type $Na_{0.66}Ni_{0.33-x}Zn_xMn_{0.67}O_2$ ($x = 0$, 0.07, 0.1) were prepared by conventional solid state method. Stoichiometric amount of acetate sources of sodium acetate $Na(OOCCH_3)_2.4H_2O$ (Alfa Aesar, 99.95%), nickel acetate $Ni(OOCCH_3)_2.4H_2O$ (Alfa Aesar 98 + %), manganese acetate $Mn(OOCCH_3)_2.4H_2O$ (Alfa Aesar, 99%), and zinc acetate $Zn(OOCCH_3).4H_2O$ (Alfa Aesar 98 + %) was used as precursor without further purification. The mixture was ball-milled by RETSCH-PM-100 GmbH Planetary ball miller at 250 rpm for 4 h with resting time of 5 min. After milling, it was kept in a vacuum oven at 120 °C for 6 h to remove acetate content; after that, samples were calcined at 950 °C at a heating rate of 3 °C/min for 12 h in inert atmosphere.

Material characterization

Crystalline phase of as-prepared samples was obtained via X-ray diffraction (XRD) analysis using the PANalytical X'pertpro diffractometer with CuKα (1.54 Å), in the range $2\theta = 10–70°$. Refinement of X-ray pattern was then carried out by Rietveld refinement (GSAS); the structure of material was visualized by VESTA software. Morphological studies with elemental mapping were performed by using scanning electron microscope (EVO18 (CARL ZEISS, German), and energy dispersive X-ray analysis was performed using EDX Quantax 200 with X Flash® 6130. The SAED pattern with lattice fringes was collected by high-resolution transmission electron microscopy (JEOL-2100-HR-TEM, Japan). All the electrochemical behaviors were tested by BCS-815/8 channels Battery cycler (Bio-Logic, France).

Electrochemical cell preparation

The test cells were prepared using the as-prepared electrodes containing 85 wt% of active material with 10 wt% of carbon black and Super P (99.99%, Alfa Aesar) and 5 wt% of poly(vinylidene fluoride) (PVdF) (Sigma-Aldrich) binder. The slurry was mixed with N-methyl-2-pyrrolidone (NMP) for several hours and then coated on aluminum (Al) foil. The electrodes were dried at 80 °C in a vacuum oven for overnight. The 2032-type half cells were assembled in an Ar-filled glove box with the as-prepared electrodes of mass about 10 mg/cm^2; herein, the sodium metal as anode with 1 M solution of $NaPF_6$ (sodium hexafluoro phosphate, 98% Sigma-Aldrich) and propylene carbonate (Alfa-Aeser 99%) as an electrolyte were used. Galvanostatic charge–discharge studies were carried out in the voltage range 1.5 to 4.5 V at 0.1 C at room temperature. Cyclic voltammetry (CV) was recorded between 1.8 and 4.2 V vs (Na^+/Na) at a scan rate of 0.1 mV s^{-1}. Electrochemical impedance spectroscopic (EIS) analysis was performed in the frequency range 10 kHz to 1 Hz.

Results and discussion

The crystalline nature of as-prepared materials P2-type $Na_{0.66}Ni_{0.33}Mn_{0.67}O_2$ and Zn-substituted P2-$Na_{0.66}Ni_{0.33-x}Zn_{1-x}Mn_{0.67}O_2$ was analyzed by X-ray diffraction analysis. The obtained diffraction patterns are showed in Fig. 1a. All the diffraction peaks can be indexed to the space group $P6_3/mmc$(No.194) with hexagonal symmetry (JCPDS #54–0894) [23] (Fig. 1a). From the refinement data, the lattice parameters of all as-prepared samples were observed (Fig. 1b–d); the change in lattice parameters while increasing the Zn content in the P2-Na-Ni-Mn-O system was observed. It is due to dependable crystal radius of Zn^{2+} (88 pm). The increased unit cell volume upon Zn substitution will be promising for larger Na ion kinetics and enhancing the electrochemical performances [24, 25]. Some of the previous reports on this material reported having impurities of ZnO in the P2-Na-Ni-Mn-O system [26], but in this work, we have obtained pure P2-Na-Ni-Mn-O system with the doping concentration of Zn at x = 0.1.

The P2-type layered structure was basically formed by sharing one half of the prism with transition metal oxide sheets (TMO_6) of octahedral layer and other half of the prism shared the faces (Fig.2) [27].

Microstructural analysis was performed on the as-prepared samples at a working distance of 11.2 mm; the SEM images are shown in Fig. 3a–c). SEM micrographs demonstrate the irregular particles with different sizes, and sequence of layer slips were observed. There was a exfoliation of sheets of layer observed on surface morphology of all the samples.

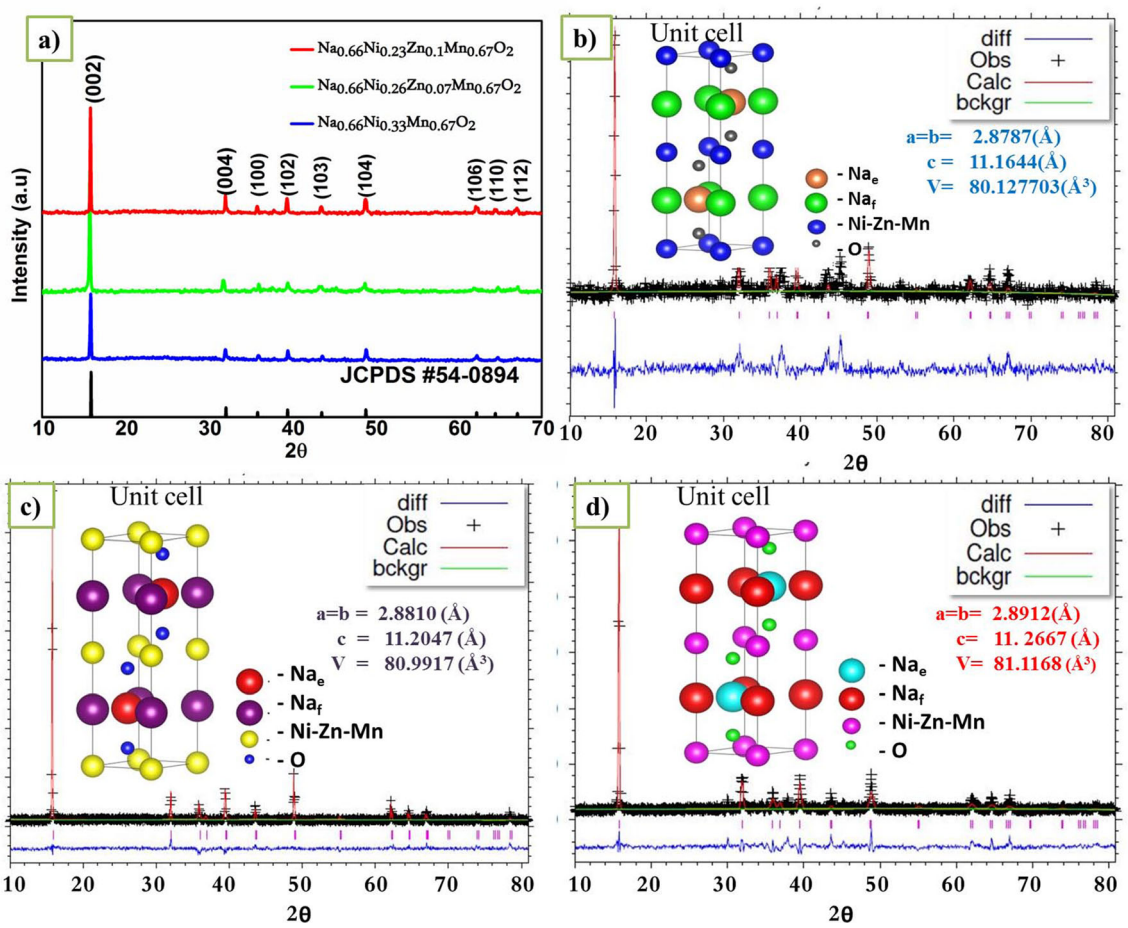

Fig. 1 **a** XRD pattern of as-prepared samples, **b–d** refinement images of P2-type $Na_{0.66}Ni_{0.33}Mn_{0.67}O_2$, P2-$Na_{0.66}Ni_{0.26}Zn_{0.07}Mn_{0.67}O_2$, and P2-$Na_{0.66}Ni_{0.23}Zn_{0.1}Mn_{0.67}O_2$, respectively (inset—unit cell)

Moreover, the layer sheets are broken with sharp edges. The high-resolution TEM mages of the prepared samples with observed grains at different scales and SAED (selected area diffraction pattern) pattern with lattice fringes are shown in Fig. 3d–i. The layer structure of material remains unchanged even after Zn doping, which was clearly confirmed through

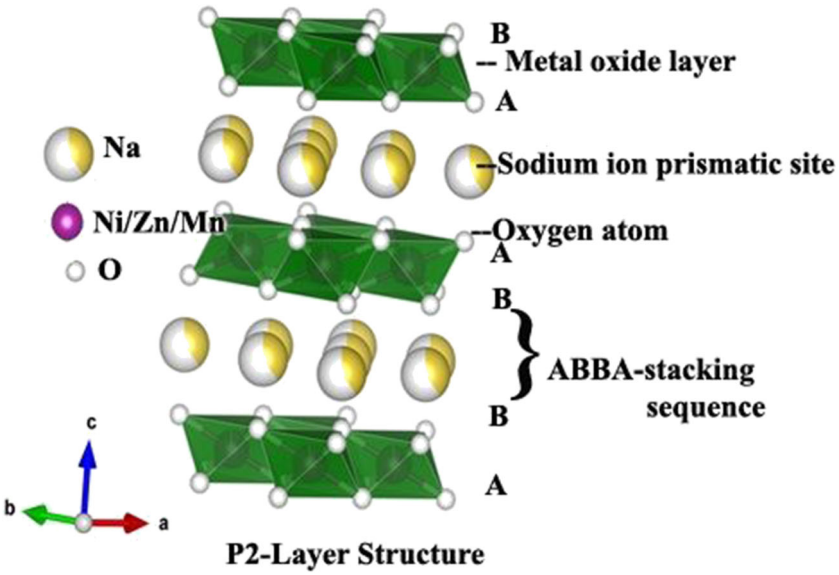

Fig. 2 Schematic representation of P2-type layered structure

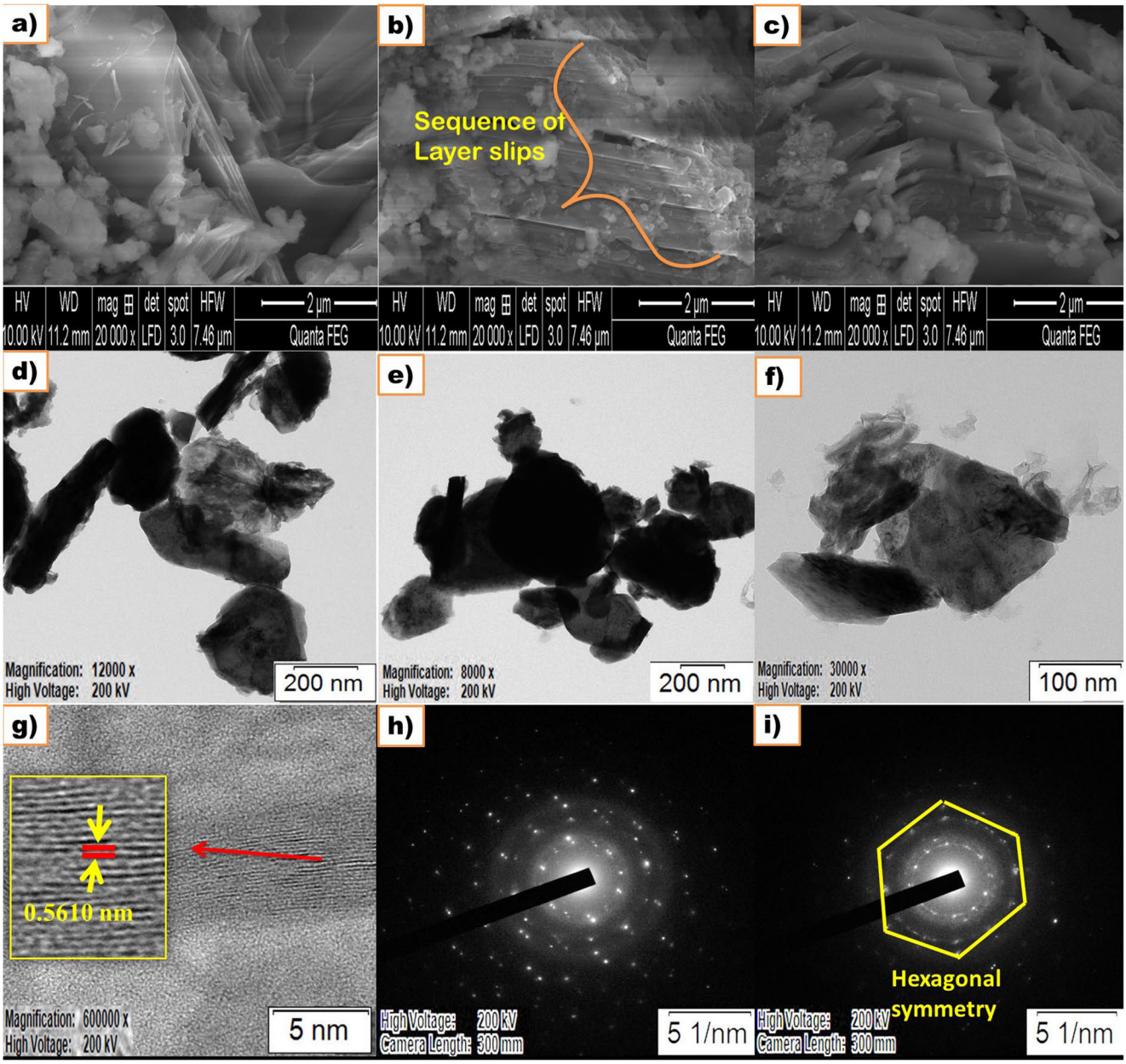

Fig. 3 **a**–**c** surface micrographs of P2-type $Na_{0.66}Ni_{0.33}Mn_{0.67}O_2$, P2-$Na_{0.66}Ni_{0.26}Zn_{0.07}Mn_{0.67}O_2$, and P2-$Na_{0.66}Ni_{0.23}Zn_{0.1}Mn_{0.67}O_2$ at 2 µm scale, respectively; **d**–**f** HR-TEM images—grain size of above samples at 100–200 nm; **g** lattice fringes of P2-$Na_{0.66}Ni_{0.23}Zn_{0.1}Mn_{0.67}O_2$ with interlayer distance of 0.56 nm; **h**, **i** SAED pattern of P2-type $Na_{0.66}Ni_{0.33}Mn_{0.67}O_2$, Zn-doped P2-$Na_{0.66}Ni_{0.23}Zn_{0.1}Mn_{0.67}O_2$

the TEM images. The inter-layer distance between the nearby lattice fringes can be well defined to the value of 0.5610 nm, which is corresponding to the *d*-spacing value of (002) plane in P2 structure (Fig. 3g) of P2-$Na_{0.66}Ni_{0.23}Zn_{0.1}Mn_{0.67}O_2$. The speckled SAED pattern clearly shows the hexagonal symmetry for P2-type layer structure before and after of Zn substitution (Fig. 3h, $Na_{0.66}Ni_{0.33}Mn_{0.67}O_2$; Fig. 3i, P2-$Na_{0.66}Ni_{0.23}Zn_{0.1}Mn_{0.67}O_2$) with corresponding to crystal plane (1010) [28, 29].Occurrence of Zn in the prepared sample and its dispersal in Na-Ni-Mn-O system were confirmed by energy dispersive X-ray microanalysis (EDX) shown in Fig. 4 (though all samples were studied, the mapping of sample has the value $x = 0.1$ is given). Mapping was carried out in the scale of 50 µm with multiple areas. The result established the even distribution of the elements as O—oxygen, Na—sodium, Mn—manganese, Ni—nickel, and Zn—zinc, respectively (Fig.4), and concluded that there are no coagulations of elements in the P2-Na-Ni-Mn-O system.

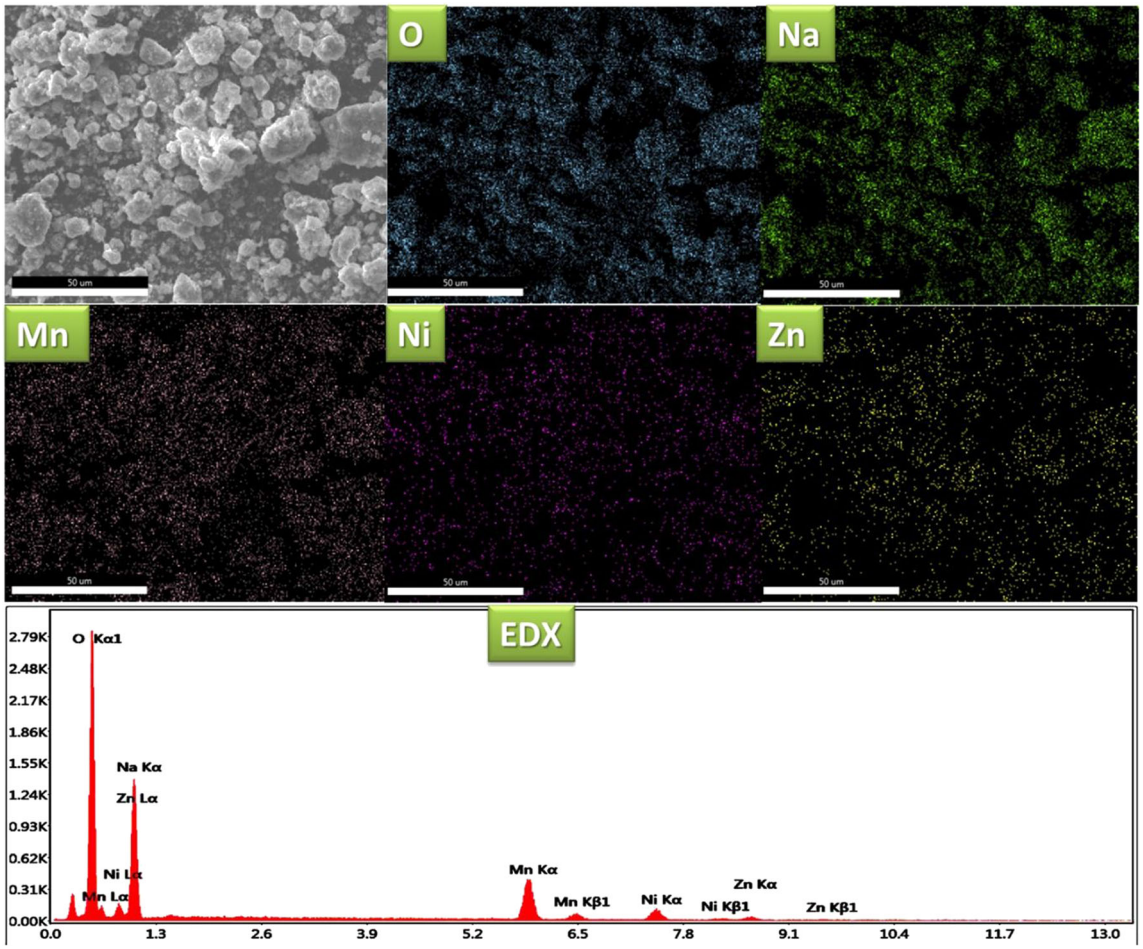

Fig. 4 Mapping images of the sample P2-$Na_{0.66}Ni_{0.23}Zn_{0.1}Mn_{0.67}O_2$ elements as O—oxygen, Na—sodium, Mn—manganese, Ni—nickel, and Zn—zinc, respectively. The EDX spectra of the P2-$Na_{0.66}Ni_{0.23}Zn_{0.1}Mn_{0.67}O_2$ show the presence of Zn in prepared sample

Electrochemical studies

Galvanostatic charge–discharge analysis was performed for the prepared samples at 0.1 C in between 1.5 and 4.5 V. The C/D plot of P2-type $Na_{0.66}Ni_{0.33}Mn_{0.67}O_2$, P2-$Na_{0.66}Ni_{0.26}Zn_{0.07}Mn_{0.67}O_2$, and P2-$Na_{0.66}Ni_{0.23}Zn_{0.1}Mn_{0.67}O_2$ is shown in Fig. 5a–c. The un-doped P2-Na-Ni-Mn-O sample delivered an initial discharge capacity of 210 mAh g^{-1} (Fig. 5a) with capacity retention around 42% for 30 cycles; there was a huge capacity fading observed when cycled at potential of 4.5 V. This capacity decay may be due to the P2-O2 phase evolution held by the sliding with enlargement of the metal oxide layers when cycled above the cut-off voltage ≥ 4.2 V [15, 30–32]. The materials cannot rearrange the initial P2-structure, which leads to defeat in sustainability upon cycling. Although the Zn-substituted P2-$Na_{0.66}Ni_{0.26}Zn_{0.07}Mn_{0.67}O_2$ delivered initial discharge capacity of 208 mAh g^{-1} (Fig. 5b), it is noticed that the capacity retention slightly increased to 55% when compared with un-doped samples. However, the sample with $x = 0.1$ exhibits 61% after 30 cycles, which is higher than all other samples. This clearly dictates that the increased Zn substitution is favorable to stabilizing the structure of P2-Na-Ni-Mn-O system [10]. Yang et al. [33] reported that the Zn-substitution would enhance the P2-O2 phase reversibility even when it was operated even at higher cut-off voltage (≥ 4.2 V) in the $Na_{0.66}Ni_{0.26}Zn_{0.07}Mn_{0.67}O_2$ system. In the present study, it is demonstrated that the P2 structure of $Na_{0.66}Ni_{0.23}Zn_{0.1}Mn_{0.67}O_2$ sample has stabled electrochemical performances at higher voltage range ≥ 4.2 V. Moreover, the reason for high capacity deliver at initial cycles beyond the theoretical value in the layered-type P2-$Na_{0.66}Ni_{0.33}Mn_{0.67}O_2$ electrodes expected to redox couple of transition metal (Ni^{+}), oxygen redox activity, and lower cut-off voltage (< 2) [34, 35]. Wang et al. [36] mentioned that the structure of P2-$Na_{0.66}Ni_{0.33}Mn_{0.67}O_2$ was dented when cycled between 2.0 and 4.5 V due to over insertion of Na^{+} and its confirmed via X-ray diffraction analysis of material before and after of charge discharge. In addition, the author claimed that the stability of the material strongly defends upon potential window of charge/discharge process. However, in this work, the structural defects were entirely unfurnished by cation (Zn) mixing

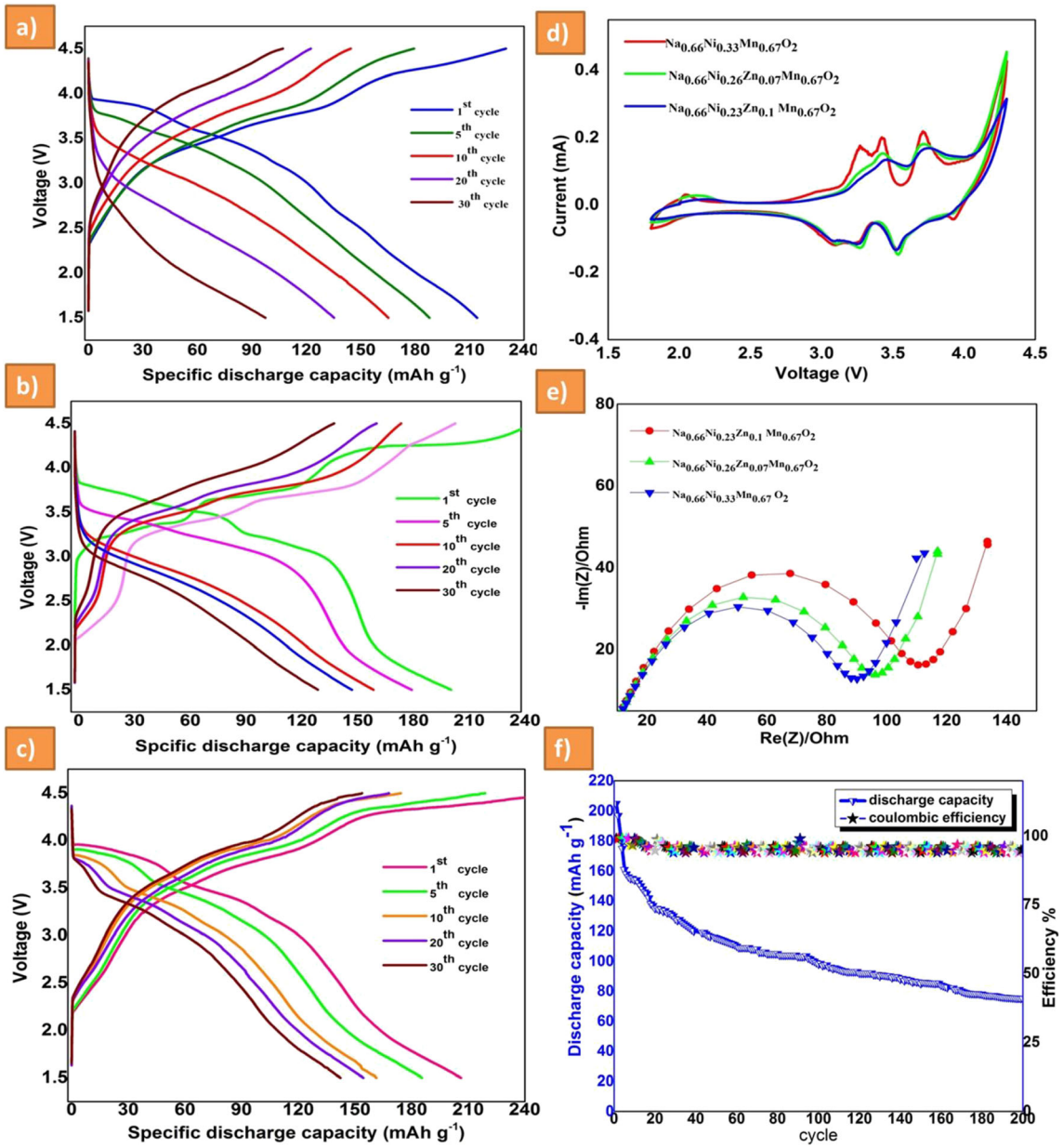

Fig. 5 **a**–**c** Charge-discharge profile of sample P2-type $Na_{0.66}Ni_{0.33}Mn_{0.67}O_2$, P2-$Na_{0.66}Ni_{0.26}Zn_{0.07}Mn_{0.67}O_2$, P2-$Na_{0.66}Ni_{0.23}Zn_{0.1}Mn_{0.67}O_2$, respectively, at 0.1 C in the range 1.5 to 4.5 V; **d** cyclic voltammetry of P2-type $Na_{0.66}Ni_{0.33}Mn_{0.67}O_2$, P2-$Na_{0.66}Ni_{0.26}Zn_{0.07}Mn_{0.67}O_2$, P2-$Na_{0.66}Ni_{0.23}Zn_{0.1}Mn_{0.67}O_2$, respectively, samples at the scan rate 0.1 mV between 1.5 and 4.5 V; **e** electrochemical impedance spectrum of prepared samples in the range 10 kHz to 10 Hz; **f** coulombic efficiency with discharge capacity plot of P2-$Na_{0.66}Ni_{0.23}Zn_{0.1}Mn_{0.67}O_2$ up to 200 cycles

with stabilized structure stability of P2-$Na_{0.66}Ni_{0.23}Zn_{0.1}Mn_{0.67}O_2$ and extended operating potential window 1.5–4.5 V. The structure stability of P2-$Na_{0.66}Ni_{0.23}Zn_{0.1}Mn_{0.67}O_2$ operated at high cut-off voltage 1.5–4.5 V was confirmed by X-ray diffraction pattern analyses of the sample after 200 C/D cycles at charged state, as shown in Supplementary Fig.S1. However, there was reduced intensity of the diffraction peaks observed, but no more change in positions of peaks was observed for P2-$Na_{0.66}Ni_{0.23}Zn_{0.1}Mn_{0.67}O_2$ cycled up to 200 cycles; these results indicate that the increased Zn content substitution into P2-Na-Ni-Mn-O system was holding the P2 structure even cycled at higher cut-off voltage range and made it as a promising electrode for practical applications. The cyclic voltammetry of the prepared samples examined at a scan rate of 0.1 mV/s at 1.8 to 4.2 V is shown in Fig. 5d. This clearly shows that all the redox peaks are broader and their current decreases with the increase of Zn content in P2-Na-Ni-Mn-O system [10]. The redox peaks above the 2.5 V are due to the redox reaction of the $Ni^{3+/}$ Ni^{2+} and Ni^{4+}/ Ni^{3+} redox pairs;

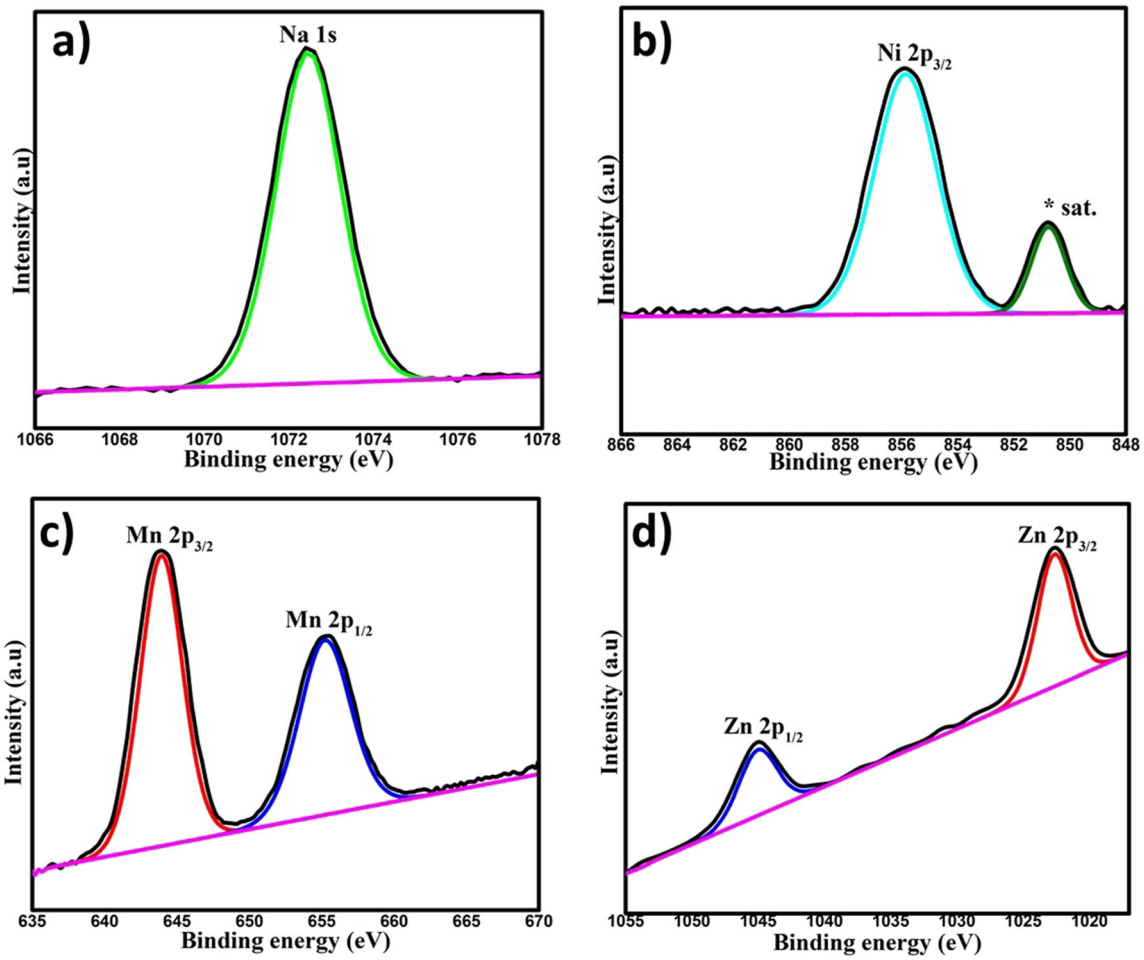

Fig. 6 XPS spectra for **a** Na, **b** Ni, **c** Mn, and **d** Zn of sample P2-$Na_{0.66}Ni_{0.23}Zn_{0.1}Mn_{0.67}O_2$

peaks below 2.5 V are attributed to redox reactions of Mn^{4+}/Mn^{3+} redox activity [36, 37]. Among the prepared samples, the P2-$Na_{0.66}Ni_{0.23}Zn_{0.1}Mn_{0.67}O_2$ exhibits appreciable columbic efficiency around 96% up to 200 cycles with capacity retention of 40% as shown in Fig. 5f.

Nyquist plots (Fig. 5e) for all the samples show the semicircle at high frequency area and inclined line in the region of low frequency; this may attribute to the prepared cells having noble ionic conduction nature. The charge transfer resistance (R_{ct}) value of the electrodes was well

Table 1 Comparison of capacity and operated voltage of various cathode materials so far reported on Na-ion batteries

No	Material	Potential window (V)	Initial capacity delivered (mAh g^{-1})	References
1	P2-$Na_{0.67}Ni_{0.23}Zn_{0.1}Mn_{0.67}O_2$	1.5–4.5	205	[This work]
	P2-$Na_{0.67}Ni_{0.26}Zn_{0.07}Mn_{0.67}O_2$	1.5–4.5	208	[This work]
	P2-$Na_{0.67}Ni_{0.33}Mn_{0.67}O_2$	1.5–4.5	210	[This work]
2	P2-$Na_{0.67}Ni_{0.23}Zn_{0.1}Mn_{0.67}O_2$	1.5–4.3	173	[40]
3	P2-$Na_{0.67}Ni_{0.26}Zn_{0.07}Mn_{0.67}O_2$	2.0–4.4	108	[26]
4	P2-$Na_{0.67}Ni_{0.26}Zn_{0.07}Mn_{0.67}O_2$	2.2–4.3	130	[32]
5	P2-$Na_{0.67}Ni_{0.26}Zn_{0.07}Mn_{0.67}O_2$	2.0–4.4	143	[10]
	P2-$Na_{0.67}Ni_{0.19}Zn_{0.14}Mn_{0.67}O_2$	2.0–4.4	100	
6	P2-$Na_{0.67}Mn_{0.95}Mg_{0.05}O_2$	1.5–4.0	175	[41]

agreed with earlier report based on this material [38]. In view of obtaining better information, the impedance analysis was performed for the sample P2-$Na_{0.66}Ni_{0.23}Zn_{0.1}Mn_{0.67}O_2$ after 200 cycles. Still, the cell containing P2-$Na_{0.66}Ni_{0.23}Zn_{0.1}Mn_{0.67}O_2$ holds the semicircle and inclined line at higher and lower frequency region (supplementary Fig. S2) with bit increased charge transfer resistance after 200 cycles. It reveals the stability of material with long-lasting ionic conduction nature, which is desirable for better life of battery.

In order to find out the surface chemical state of the prepared sample, it was analyzed by X-ray photoelectron spectroscopy (XPS). The oxidation state of Na, Mn, Ni, and Zn on the surface of sample is shown in Fig. 6a–d. In Fig. 6a, b, the Na at 1 s spectra in the corresponding binding energy value of 1072 eV and Mn 2p spectra shows bands at 642.9 and 654.1 eV for Mn $2p_{3/2}$ and $2p_{1/2}$, respectively. They reveal the oxidation state of Mn^{4+} [38]. The 2p spectra for Ni located in the band 854.7 eV belonging to Ni $2p_{3/2}$ with their corresponding satellite band 850.4 and hat positions are well matched with Ni^{2+} [39]. The Zn $2p_{3/2}$ peaks appear at 1022.4 eV for the Zn-substituted sample ($x = 0.1$) in divalent state. Finally, those results evident the oxidation state of the Mn; Ni did not change after substitution of Zn in to the host P2-type material (Table 1) [26].

Conclusion

The P2-type Na-Ni-Mn-O, P2-$Na_{0.67}Ni_{0.26}Zn_{0.07}Mn_{0.67}O_2$, and P2-$Na_{0.67}Ni_{0.23}Zn_{0.1}Mn_{0.67}O_2$ electrode materials have been successfully prepared by the conventional solid state method, and all studies were performed as well. This work was originated to overcome the drawbacks of the P2-Na-Ni-Mn-O system, by substituting Zn in to it. It is clearly visible from the obtained results that Zn substitution strongly overcomes the structural drawbacks of the P2-Na-Ni-Mn-O system. Therefore, the P2-Na-Ni-Mn-O system can uphold its structure while cycling at higher cut-off potential range, which turns this material towards the possible practical application. From the XRD and XPS results, it is confirmed that the Zn substitution does not affect the P2-layer structure. To the best of our knowledge, we report the maximum discharge capacity of 205 mAh g^{-1} for P2-$Na_{0.67}Ni_{0.23}Zn_{0.1}Mn_{0.67}O_2$ at extended ($\geq$4.2 V) operating potential window of 1.5–4.5 V for this system. The long-lasting electrochemical performances with appreciable efficiency are to be notable one. Therefore, Zn-doped P2-Na-Ni-Mn-O-based electrode can be served as the best one for sodium ion battery.

Acknowledgments All the authors gratefully acknowledge the extending of the analytical facilities in the Department of Physics, Alagappa University, under the PURSE and FIST program, sponsored by Department of Science and Technology (DST) New Delhi, Govt. of India and Ministry of Human Resource Development RUSA Phase 2.0 grant sanctioned vide Lt.No.F-24-51/2014 U Policy (TNMulti Gen), Dept. of Education, Govt. of India.

Author contributions All the authors equally contributed in terms of framing, planning, and executing this research work, analytical and writing parts too.

Funding information All the authors from Alagappa University received financial support from DST-SERB, New Delhi, under the Physical Sciences, grant sanctioned vide EMR/2016/006302.

Compliance with ethical standards

Competing interests All the authors declare that they have no competing interests.

I assure that this manuscript was not previously submitted to any journal for publication.

I assure that the manuscript or its contents in some other form have not been published previously by any of the authors and/or is not under consideration for publication in another journal at the time of submission.

References

1. Huang Y, Li X, Wang J, Miao L, Li C, Han J, Huang Y (2018) Superior Na-ion storage achieved by Ti substitution in $Na_3V_2(PO_4)_3$. Energy Storage Mater 15:108–115
2. Chen C, Wen Y, Hu X, Ji X, Yan M, Mai L, Hu P, Shan B, Huang Y (2015) Na^+ intercalation pseudocapacitance in graphene-coupled titanium oxide enabling ultra-fast sodium storage and long-term cycling. Nat Commun 6:6929
3. Huang Y, Li X, Luo J, Wang K, Zhang Q, Qiu Y, Sun S, Liu S, Han J, Huang Y (2017) Enhancing sodium-ion storage behaviors in $TiNb_2O_7$ by mechanical ball milling. ACS Appl Mater Interfaces 9(10):8696–8703
4. Nayak PK, Erickson EM, Schipper F, Penki TR, Munichandraiah N, Adelhelm P, Sclar H, Amalraj F, Markovsky B, Aurbach D (2018) Review on challenges and recent advances in the electrochemical performance of high capacity Li-and Mn-rich cathode materials for Li-ion batteries. Adv Energy Mater 8(8):1702397
5. Kim SW, Seo DH, Ma X, Ceder G, Kang K (2012) Electrode materials for rechargeable sodium-ion batteries: potential alternatives to current lithium-ion batteries. Adv Energy Mater 2(7):710–721
6. Pan H, Hu YS, Chen L (2013) Room-temperature stationary sodium-ion batteries for large-scale electric energy storage. Energy Environ Sci 6(8):2338–2360
7. Yabuuchi N, Kubota K, Dahbi M, Komaba S (2014) Research development on sodium-ion batteries. Chem Rev 114(23):11636–11682
8. Slater MD, Kim D, Lee E, Johnson CS (2013) Sodium-ion batteries. Adv Funct Mater 23(8):947–958
9. Sathiya M, Hemalatha K, Ramesha K, Tarascon JM, Prakash AS (2012) Chem Mater 24:1846–1853
10. Wu X, Guo J, Wang D, Zhong G, McDonald MJ, Yang Y (2015) P2-type $Na_{0.66}Ni_{0.33-x}Zn_xMn_{0.67}O_2$ as new high-voltage cathode materials for sodium-ion batteries. J Power Sources 281:18–26
11. Wang XF, Tamaru M, Okubo M, Yamada A (2013) J Phys Chem C 117:15545–15551
12. Buchholz D, Chagas LG, Vaalma C, Wu LM, Passerini S (2014) J Mater Chem A 213415–213421

13. Cheng JH, Pan CJ, Lee JF, Chen JM, Guignard M, Delmas C, Carlier D, Hwang BJ (2014) Simultaneous reduction of Co3+and Mn4+in P2-Na2/3Co2/3Mn1/3O2 as evidenced by X-ray absorption spectroscopy during electrochemical sodium intercalation. Chem Mater 26:1219–1225
14. Komaba S, Yabuuchi N, Nakayama T, Ogata A, Ishikawa T, Nakai I (2012) Study on the reversible electrode reaction of Na1–xNi0.5Mn0.5O2 for a rechargeable sodium-ion battery. Inorg.Chem. 51:6211–6220
15. Lee DH, Xu J, Meng YS (2013) An advanced cathode for Na-ion batteries with high rate and excellent structural stability. Phys Chem Chem Phys 15(9):3304–3312
16. Hwang JY, Myung ST, Choi JU, Yoon CS, Yashiro H, Sun YK (2017) Resolving the degradation pathways of the O3-type layered oxide cathode surface through the nano-scale aluminum oxide coating for high-energy density sodium-ion batteries. J Mater Chem A 5(45):23671–23680
17. Wang QY, Liu J, Murugan AV, Manthiram A (2009) High capacity double-layer surface modified $Li[Li_{0.2}Mn_{0.54}Ni_{0.13}Co_{0.13}]O_2$ cathode with improved rate capability. *J Mater Chem* 19(28):4965–4972
18. Buchholz D, Chagas LG, Winter M, Passerini S (2013) P2-type layered Na0.45Ni0.22Co0.11Mn0.66O2 as intercalation host material for lithium and sodium batteries. Electrochim Acta 110:208–213
19. Yuan DD, Hu XH, Qian JF, Pei F, Wu FY, Mao RJ, Ai XP, Yang HX, Cao YL (2014) P2-type Na0.67Mn0.65Fe0.2Ni0.15O2 cathode material with high-capacity for sodium-ion battery. Electrochim Acta 116:300–305
20. Kim DH, Kang SH, Slater M, Rood S, Vaughey JT, Karan N, Balasubramanian M, Johnson CS (2011) Enabling sodium batteries using lithium-substituted sodium layered transition metal oxide cathodes. Adv Energy Mater 1:333–336
21. Xu J, Lee DH, Clement RJ, Yu XQ, Leskes M, Pell AJ, Pintacuda G, Yang XQ, Grey CP, Meng YS (2014) Chem Mater 26:1260–1269
22. Yoshida H, Yabuuchi N, Kubota K, Ikeuchi I, Garsuch A, Schulz-Dobrick M, Komaba S (2014) P2-type Na2/3Ni1/3Mn2/3−xTixO2 as a new positive electrode for higher energy Na-ion batteries. Chem Commun 50:3677–3680
23. Paulsen J, Donaberger R, Dahn J (2000) Chem Mater 12:2257–2267
24. Saroha R, Panwar AK, Sharma Y, Tyagi PK, Ghosh S (2017) Development of surface functionalized ZnO-doped $LiFePO_4$/C composites as alternative cathode material for lithium ion batteries. Appl Surf Sci 394:25–36
25. Lee YS, Ryu KS (2017) Study of the lithium diffusion properties and high rate performance of $TiNb_6O_{17}$ as an anode in lithium secondary battery. Sci Rep 7(1):16617
26. Zuo W, Liu R, Ortiz GF, Rubio S, Chyrka T, Lavela P, Zheng S, Tirado JL, Wang D, Yang Y (2018) Sodium storage behavior of $Na_{0.66}Ni_{0.33-x}Zn_xMn_{0.67}O_2$ (x= 0, 0.07 and 0.14) positive materials in diglyme-based electrolytes. J Power Sources 400:317–324
27. Delmas C, Fouassier C, Hagenmuller P (1980) Structural classification and properties of the layered oxides. Physica B+ c 99(1–4):81–85
28. Lu Z, Donaberger RA, Dahn JR (2000) Superlattice ordering of Mn, Ni, and Co in layered alkali transition metal oxides with P2, P3, and O3 structures. Chem Mater 12(12):3583–3590
29. Luo LB, Zhao YG, Zhang GM, Guo SM, Li Z, Luo JL (2007) Spin-glass behavior in hexagonal $Na_{0.70}MnO_2$. Phys Rev B 75(12):125115
30. Komaba S, Yabuuchi N, Nakayama T, Ogata A, Ishikawa T, Nakai I (2012) Study on the reversible electrode reaction of $Na_{1-x}Ni_{0.5}Mn_{0.5}O_2$ for a rechargeable sodium-ion battery. Inorg Chem 51(11):6211–6220
31. Yoshida H, Yabuuchi N, Kubota K, Ikeuchi I, Garsuch A, Schulz-Dobrick M, Komaba S (2014) P2-type Na2/3Ni1/3Mn2/3−xTixO2as a new positive electrode for higher energy Na-ion batteries. Chem Commun J Chem Soc Sect D 50:3677–3680
32. Wu X, Xu GL, Zhong G, Gong Z, McDonald MJ, Zheng S, Fu R, Chen Z, Amine K, Yang Y (2016) Insights into the effects of zinc doping on structural phase transition of P2-type sodium nickel manganese oxide cathodes for high-energy sodium ion batteries. ACS Appl Mater Interfaces 8(34):22227–22237
33. Risthaus T, Zhou D, Cao X, He X, Qiu B, Wang J, Zhang L, Liu Z, Paillard E, Schumacher G, Winter M (2018) A high-capacity P2 $Na_{2/3}Ni_{1/3}Mn_{2/3}O_2$ cathode material for sodium ion batteries with oxygen activity. J Power Sources 395:16–24
34. Wang H, Yang B, Liao XZ, Xu J, Yang D, He YS, Ma ZF (2013) Electrochemical properties of P2-$Na_{2/3}$ $[Ni_{1/3}Mn_{2/3}]$ O_2 cathode material for sodium ion batteries when cycled in different voltage ranges. Electrochim Acta 113:200–204
35. Wang PF, Yao HR, Liu XY, Yin YX, Zhang JN, Wen Y, Yu X, Gu L, Guo YG et al (2018) Sci Adv 4(3):eaar6018
36. Hasa I, Buchholz D, Passerini S, Hassoun J (2015) A comparative study of layered transition metal oxide cathodes for application in sodium-ion battery. ACS Appl Mater Interfaces 7(9):5206–5212
37. Wu XB, Wang SH, Lin XC, Zhong GM, Gong ZL, Yang Y (2014) J Mater Chem A 2:1006–1013
38. Yan G, Li X, Wang Z, Guo H, Xiong X (2014) Beneficial effects of 1-propylphosphonic acid cyclic anhydride as an electrolyte additive on the electrochemical properties of $LiNi_{0.5}Mn_{1.5}O_4$ cathode material. J Power Sources 263:231–238
39. Lee JH, Kim KJ (2014) Structural and electrochemical evolution with post-annealing temperature of solution-based $LiNi_{0.5}Mn_{1.5}O_4$ thin-film cathodes for microbatteries with cyclic stability. Electrochim Acta 137:169–174
40. Hong JH, Wang MY, Du YY, Deng L, He G (2019) The role of Zn substitution in P2-type $Na_{0.67}Ni_{0.23}Zn_{0.1}Mn_{0.67}O_2$ cathode for inhibiting the phase transition at high potential and dissolution of manganese at low potential. J Mater Sci Mater Electron 30(4):4006–4013
41. Billaud J, Singh G, Armstrong AR, Gonzalo E, Roddatis V, Armand M, Rojo T, Bruce PG (2014) $Na_{0.67}Mn_{1-x}Mg_xO_2$ ($0 \leq x \leq 0.2$): a high capacity cathode for sodium-ion batteries. Energy Environ Sci 7(4):1387–1391